PAMUKKALE ÜNİVERSİTESİ
Mühendislik Bilimleri Dergisi

PAMUKKALE UNIVERSITY
Journal of Engineering Sciences

Araştırma makalesi | Research paper

Cilt | Vol: XX • Sayı | No: X • ss | pp: XXXX-XXXX • Yıl | Year: 20XX

Effect of process parameters and annealing treatment on mechanical and surface properties of PLA samples

Gökhan Haydarlar, Tevfik Oğuzhan Ergüder, Semih Duran

ARTICLE INFO

Dates:
Received: 13.01.2026
Accepted: 10.04.2026

Doi:
10.65206/pajes.1862801

Corresponding author:
Semih Duran
(semih.duran@kafkas.edu.tr)

Author addresses:
Department of Mechanical Engineering, Faculty of Engineering and Architecture, Kafkas University, Kars, 36100 Türkiye
(gokhan.haydarlar@kafkas.edu.tr; oguzhan.erguder@kafkas.edu.tr; semih.duran@kafkas.edu.tr)

ABSTRACT

Context—Fused Deposition Modeling (FDM) has become a commonly adopted additive manufacturing method because it offers economical production, geometric versatility, and broad material availability. Among the thermoplastics used in FDM, polylactic acid (PLA) is widely preferred due to its environmentally friendly nature and favorable processing characteristics. Nevertheless, the mechanical properties and surface finish of PLA parts produced by FDM are highly sensitive to both manufacturing parameters and post-processing practices. Although previous research has reported the separate effects of factors such as layer thickness, infill density, and annealing, studies that systematically evaluate their combined impact are still scarce.

Objective—This research focused on examining how variations in layer thickness, infill density, and annealing temperature affect the tensile performance and surface characteristics of PLA parts produced by FDM. In particular, the study aimed to determine which processing parameters most strongly influence tensile strength, elastic modulus, elongation, specific tensile strength, and surface roughness, as well as to explain their role in balancing stiffness and ductility in printed PLA parts.

Method—An L9 Taguchi orthogonal array was implemented to assess the influence of layer thickness set at 0.12, 0.16, and 0.20 mm, infill density levels of 20, 40, and 60 percent, and annealing states consisting of as-printed, 60°C, and 90 °C. Tensile samples made of PLA were fabricated using an FDM-based 3D printing system under controlled processing conditions. Mechanical characterization was carried out through tensile testing to obtain tensile strength, elastic modulus, and elongation values, whereas specific tensile strength was determined by incorporating sample mass measurements. Surface quality was evaluated by measuring the average surface roughness (Ra) with a three-dimensional optical profilometer. The effects and relative significance of the selected parameters were statistically analyzed using signal-to-noise ratios and analysis of variance techniques.

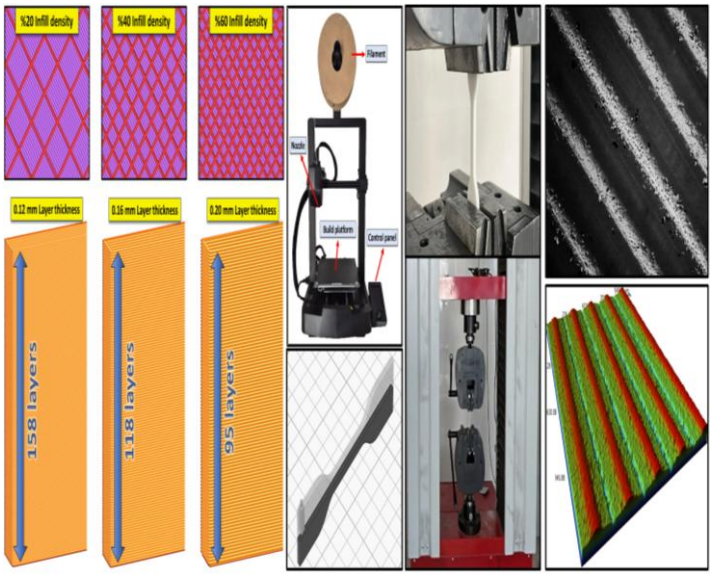

Results—The results showed that infill density was the most important factor affecting tensile strength, with a contribution ratio of 87.76%, and maximum strengths of approximately 43–45 MPa obtained at 60% infill. Layer thickness was identified as the dominant parameter controlling elastic modulus (48.17%) and elongation (71.64%), its critical role in the stiffness–ductility balance. Surface roughness increased as thicker layers formed more pronounced and visible layer-step structures. Surface roughness increased as thicker layers produced more pronounced and visible layer-step structures. The overall effect of layer thickness on surface roughness was 84.73%.

Conclusion—This work presents an integrated assessment of how multiple processing parameters influence the mechanical behavior and surface characteristics of PLA components. The results support the optimization of strength, ductility, weight efficiency, and surface finish, and contribute practical insight for the engineering design of PLA parts manufactured by FDM.

Key Words—FDM, PLA, Mechanical properties, Surface roughness

I. INTRODUCTION

Additive manufacturing (AM) is a production method that enables the layer-by-layer fabrication of objects from three-dimensional (3D) CAD models, serving as an alternative to conventional manufacturing techniques [1]–[3]. The direct production of functional end-use components via additive manufacturing (AM) has seen broad adoption across critical industries, notably aerospace [4], automotive [5], and medical applications [6]. Within the AM landscape, techniques such as selective laser sintering (SLS) and selective laser melting (SLM) provide components with excellent mechanical properties. However, their high equipment costs restrict widespread accessibility. In contrast, the material extrusion-based Fused Deposition Modeling (FDM) method has gained prominence as the most ubiquitous AM technology, primarily due to its economic feasibility and user-friendly operation [7]–[9]. The FDM process fundamentally involves the controlled deposition of a semi-molten thermoplastic filament through a heated nozzle onto a build platform, constructing objects sequentially [10]–[12]. Although FDM benefits from extensive material options and cost-effectiveness, the resultant mechanical performance of fabricated parts is a complex function not only of the base polymer but also critically of the employed printing parameters [13]–[16]. Polylactic Acid (PLA) is the dominant thermoplastic polymer in FDM applications, widely favored for its low cost, excellent processability, and biodegradable nature, making it a suitable candidate for sustainable manufacturing initiatives [17], [18]. Its low melting temperature and low glass transition temperature (Tg ≈ 55–65°C) facilitate the printing process by minimizing part warping during production [19]–[21]. However, PLA exhibits inherently high brittleness and low thermal stability. Consequently, achieving enhanced mechanical properties in PLA parts necessitates the meticulous optimization of printing conditions coupled with strategic post-processing thermal treatments [22], [23].

Layer reach is one of the most fundamental factors affecting breakage in the FDM printing process. This parameter, by controlling the height of a layer, directly impacts not only mechanical performance but also surface roughness and geometric appearance [24]–[26]. Studies reported in the literature generally showed that samples produced with thinner layers using the FDM method exhibited higher tensile strength due to improved interlayer bonding [27], [28]. Rodríguez-Panes et al.'s study revealed that increasing the layer thickness in PLA material leads to approximately an 11% decrease in maximum tensile strength [29]. Previous experimental studies have clearly shown that layer thickness plays a critical role in determining the tensile properties of PLA materials. For example, Kiński et al. reported that increasing the layer height from 0.1 mm to 0.3 mm resulted in an approximately 20% reduction in tensile strength [30]. A similar trend was quantified by Anoop et al., whose results indicated a more pronounced reduction of up to 28% in tensile strength with increased layer thickness [31]. However, the mechanical trade-offs related to this parameter were complex. Contrasting with these findings, Jatti et al. noted that although thicker layers diminished tensile properties, they concurrently enhanced impact resistance and flexural strength, highlighting a critical balance in mechanical design [32]. These studies showed that at lower layer thicknesses, layers adhered more densely to each other, and a stronger diffusion bond was formed.

Beyond the printing geometry defined by layer thickness, the internal structure determined by infill density is a critical determinant of the final part's mechanical behavior. Research by Garg et al. established a direct positive correlation, where elevating the infill density from 20% to 100% led to a marked enhancement in tensile strength [33]. Similarly, Santosh et al. quantified this relationship further, demonstrating that boosting the infill density from 25% to 100% produced a dramatic 168% improvement in tensile strength. This substantial gain, however, came with a consequential trade-off: a 20.34% reduction in material elongation, underscoring the inverse relationship between strength and ductility in this context [34]. In similar studies performed on PLA samples, it was stated that mechanical properties improved with increasing infill density and that flexural strength in particular showed a significant improvement [35],[36]. In addition, Mishra et al. indicated that impact strength reached its maximum value at an infill level of 85%, whereas infill densities above this level could negatively affect impact resistance [37]. In summary, these findings showed that increasing the infill density enhanced the mechanical strength of the produced parts but could lead to adverse effects in terms of ductility. Therefore, the optimum infill density needs to be determined depending on the application.

PLA materials produced using the FDM method generally exhibit a semi-stable and amorphous structure due to rapid cooling. The heat treatment process applied to improve the microstructure of the material and increase its crystallinity is one of the most effective methods for enhancing mechanical performance [38]–[40]. Kartal et al., who investigated the annealing of PLA samples at 85°C for 90 minutes, reported that this process resulted in increases of 48% in tensile stress and 78% in elastic modulus [41]. Pazhamannil et al. detected a 25.26% increase in ultimate tensile strength after annealing at 95°C [42]. Evaluating the effect of annealing through microstructural transformations, Reis et al. demonstrated that the transformation of amorphous regions into crystalline structures led to an increase in elastic modulus in the range of 26–51% [43]. However, Jayanth et al. reported that heat treatment performed at 80°C increased tensile strength by 20% but caused an about 10% decrease in elastic modulus [44]. Accordingly, a review of the literature confirms that the selected annealing temperature is a pivotal factor determining the crystalline morphology and resultant mechanical characteristics of PLA components. Optimal property enhancement is typically obtained when the heat treatment is conducted at or slightly above the material's glass transition temperature (Tg). In contrast, the application of temperatures that deviate significantly from this optimal range can induce adverse effects, ultimately leading to a deterioration in overall performance.

Although earlier research has examined the individual effects of layer thickness, infill density, and annealing treatments, studies that simultaneously assess these parameters together and their combined effect on the mechanical behavior of PLA components are still limited. Also, the interaction between manufacturing parameters and surface-related characteristics, particularly surface roughness, has not been sufficiently addressed in the literature, nor has its combined influence on mechanical performance been comprehensively discussed. The novelty of the present study lies in the integrated and statistically systematic evaluation of mechanical properties and surface roughness of PLA parts by simultaneously considering printing parameters and annealing effects within a single Taguchi-based experimental framework. Unlike most previous studies that focus on either mechanical behavior or surface characteristics independently, this work yields a combined optimization-oriented perspective. In this work, the tensile properties and surface roughness of FDM-fabricated PLA parts were systematically investigated by varying layer thickness, infill density, and annealing temperature according to a Taguchi L9 orthogonal experimental design. Samples produced under different parameter combinations were subjected to tensile testing to obtain key mechanical properties such as elastic modulus, tensile strength, and elongation. Surface roughness measurements were also performed to assess changes in surface morphology resulting from processing conditions. Statistical evaluations based on S/N ratios and contribution analyses were employed to identify the relative importance of each parameter on both mechanical performance and surface quality. The outcomes of this study provide valuable insight for

the design and optimization of PLA-based components intended for demanding engineering applications, including lightweight structural elements for unmanned aerial vehicles, automotive interiors and functional parts, aerospace-related systems, and precision mechanical assemblies where both mechanical reliability and surface quality are critical.

II. METHOD

Tensile test samples were designed using SolidWorks software and subsequently imported into Creality Print 6.3 for processing. Based on the predefined printing parameters, the models were prepared through slicing, and fabrication was carried out using a Creality Ender 3 V3 SE FDM-based 3D printer. To maintain consistency and enable reliable comparison of results, the primary printing conditions were kept constant, and three samples were produced for each experimental condition. A grid-type infill pattern was applied to all samples, while the printing speed, cooling conditions, and extrusion temperature were intentionally fixed in order to isolate the effects of the selected control parameters and to preserve the statistical efficiency of the Taguchi L9 orthogonal design. The printing speed was fixed at 180 mm/s, while the cooling fan operated at 100%. The number of top and bottom layers was set to four, with two perimeter walls. The build plate temperature was maintained at 55°C, and the nozzle temperature was adjusted to 215°C. All samples were fabricated using white PLA+HS filament.

A Taguchi L9 orthogonal array was employed to assess the influence of the selected processing parameters. The selected parameters were chosen to represent geometric, structural, and post-processing thermal influences in FDM. Other processing variables were maintained constant to ensure statistical clarity and controlled evaluation within the L9 design framework. For PLA material, the glass transition temperature (Tg) is generally reported to be around 60°C, while cold crystallization typically occurs near 90°C [45], [46]. Accordingly, these temperatures were chosen for the annealing processes. The influence of layer thickness, infill density, and annealing temperature on the mechanical performance of the printed samples was then examined. In addition, S/N ratios and ANOVA analyses were used to identify the most dominant manufacturing parameters affecting tensile strength, elastic modulus, elongation, and surface roughness. The sample nomenclature and the details of the Taguchi experimental plan were presented in Table 1.

All test samples were modeled according to the ASTM D638 Type IV geometry specified in the relevant tensile testing standard and manufactured with a constant thickness of 3.2 mm to ensure reliable mechanical characterization. Schematic illustrations depicting the infill density configurations and layer thickness variations of the printed samples were provided in Fig. 1(a) and Fig. 1(b), respectively. Furthermore, the FDM 3D printer employed in the fabrication process is shown in Fig. 1(c), while the orientation of the samples on the build platform during printing is illustrated in Fig. 1(d).

In the experimental design, controlled annealing treatments were applied to all samples except S1, S6, and S8 at the specified temperatures for 1 hour, and the cooling process was carried out

Table 1. Taguchi experimental design and sample nomenclature.

Sample	Layer thickness (mm)	Infill density (%)	Annealing temperature (°C)
S1	0.12	20	As-printed
S2	0.12	40	60
S3	0.12	60	90
S4	0.16	20	60
S5	0.16	40	90
S6	0.16	60	As-printed
S7	0.20	20	90
S8	0.20	40	As-printed
S9	0.20	60	60

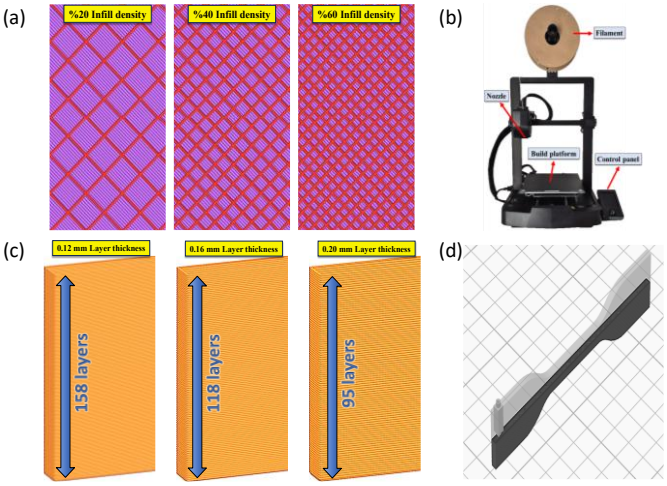

Figure 1. Printing parameters and setup (a) Infill density, (b) Layer thickness, (c) 3D printer, (d) Building orientation.

inside the furnace. A Memmert UN55 heat treatment furnace with a temperature accuracy of 0.1°C was used for the annealing processes. Following the completion of the manufacturing process, the masses of the samples were measured using a precision balance to determine the specific tensile strength in MPa/g, and the average sample weights were given in Table 2.

To determine the effects of the manufacturing variables on surface quality, surface roughness values were recorded, and optical microscope images were obtained using a Bruker Contour GT 3D profilometer. The analyses were conducted using Vision64 software. The arithmetic mean surface roughness (Ra), defined according to ISO 4287, was selected as the surface roughness criterion. Instead of a line-based profile measurement, area-based roughness measurements were carried out over a scanned surface area of 1 mm^2 in order to obtain a more representative evaluation of the characteristic layer-step morphology of FDM-fabricated PLA samples. The measurements were taken from the wide side surfaces of the samples, where the layer boundaries were directly exposed. For each sample, surface roughness measurements were performed on three different regions, and the average Ra value was reported.

Subsequently, tensile tests were conducted on the produced samples using a BESMAK tensile testing machine shown in Fig. 2 to examine their behavior under uniaxial loading. During the tests, a constant crosshead speed of 5 mm/min was applied. All experiments were carried out at room temperature under standard laboratory conditions to minimize environmental variability. During the tensile testing process, the applied load and displacement values were recorded in real time, and load–displacement curves were acquired from these data. By analyzing the obtained curves, the elastic modulus, tensile strength, and elongation values of the material were calculated. These values provided critical information for evaluating the effects of the manufacturing parameters on the mechanical performance of the samples.

III. RESULTS and DISCUSSION

The results obtained from the tensile tests were evaluated in the mechanical properties section, where tensile strength, elastic modulus, and elongation were analyzed in relation to the selected processing parameters. The findings from the 3D profilometer and optical microscopy images were discussed separately in the surface quality section, with emphasis on surface roughness and morphological characteristics.

Table 2. The average weight of samples.

Samples	S1	S2	S3	S4	S5	S6	S7	S8	S9
Weight (g)	4.55	5.02	5.43	4.34	4.75	5.16	4.27	4.77	5.25

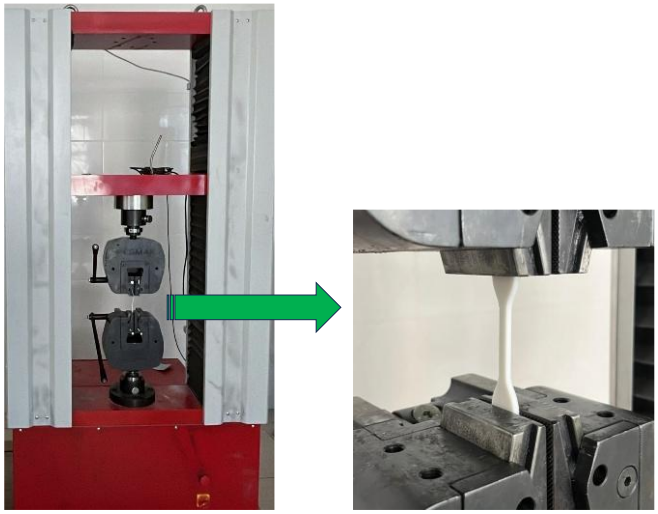

Figure 2. Detailed view of the tensile test.

A. Mechanical properties

The load–displacement curves of the manufactured tensile samples were presented in Fig. 3. Examination of the curves showed that, for all samples, the load initially exhibited an approximately linear relationship with displacement, and a decrease in load-carrying capacity occurred after reaching the maximum load. Significant differences were identified among samples produced with different processing parameters in terms of both the maximum load levels and the displacement at break.

It was determined that the maximum load values carried by the samples generally increased with increasing infill density. Samples with a 60% infill density (S3, S6, and S9) exhibited higher load-carrying capacities. This clearly indicated that the increase in material content within the internal structure enabled more effective load transfer [47], [48]. When layer thickness was evaluated, samples produced with a layer thickness of 0.12 mm showed higher slopes in the elastic region due to improved interlayer bonding [49], [50]. The annealing treatment was also found to influence the load–displacement behavior. Compared to as-printed samples, annealed samples exhibited noticeable differences in both maximum load levels and deformation behavior. The increase in maximum load observed in some samples after annealing could be attributed to the reduction of residual stresses and the rearrangement of the crystalline structure, which positively affected mechanical performance [51], [52]. Using the results obtained from the load–displacement

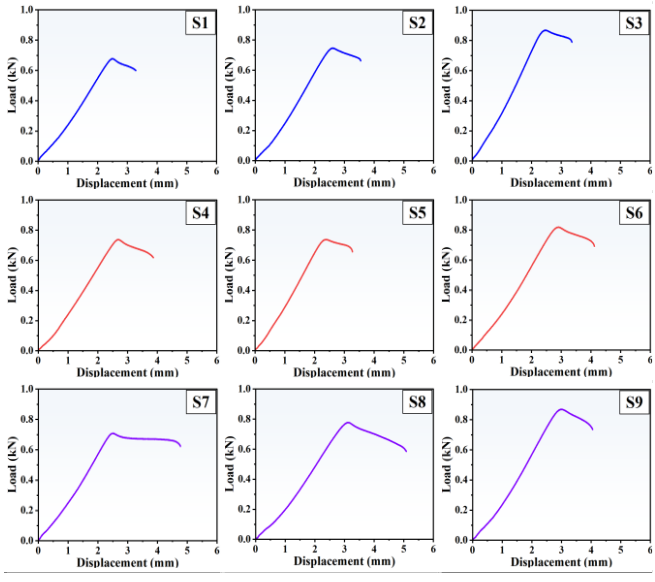

Figure 3. Load-displacement graphs of samples.

graphs, the values of elastic modulus, tensile strength, and elongation were calculated using (1)–(6). In these equations, F is the applied load, A_0 is the initial cross-sectional area of the samples, σ is the stress, Δl is the elongation amount (change in length), l_0 is the initial distance between the clamping jaws of the tensile testing machine prior to loading, ε is the strain, and E is the elastic modulus. The max. tensile strength σ_{ts} was determined using the maximum load value (F_{max}) reached during the test. In addition, the strain at break (ε_{break}) was calculated using the elongation at fracture (Δl_{break}), and the percentage elongation was obtained accordingly. In these calculations, the initial cross-sectional area of the samples was kept constant at 19.2 mm².

$$\sigma = F/A_0 \quad (1)$$

$$\varepsilon = \Delta l/l_0 \quad (2)$$

$$\sigma = E.\varepsilon \quad (3)$$

$$\sigma_{ts} = F_{max}/A_0 \quad (4)$$

$$\varepsilon_{break} = \Delta l_{break}/l_0 \quad (5)$$

Figure 4 presented the elastic modulus, tensile strength, and elongation values of all samples together with their corresponding S/N plots. The ANOVA results for tensile test were also shown in detail in Table 3. S/N analyses were performed using the larger is better approach for elastic modulus, tensile strength, and elongation. The highest tensile strength values reached approximately 43–45 MPa for samples S3, S6, and S9. With increasing infill density, the improved material continuity within the internal structure enabled a more uniform load distribution, resulting in higher maximum stress values before fracture. The mechanical property values obtained in this study were also evaluated in the context of the typical mechanical behavior of PLA materials. In the literature, tensile strength values of FDM-fabricated PLA parts are commonly reported in the range of approximately 30–60 MPa depending on printing parameters and build orientation [3], [12], [16]. The maximum tensile strength values achieved in this study (approximately 43–45 MPa) fall within this range, indicating that the selected processing conditions enabled mechanically efficient PLA structures. Examination of the S/N plots clearly showed that the infill density was the most dominant parameter affecting tensile strength. According to the ANOVA results, the contribution of infill density to tensile strength was calculated as 87.76%. In contrast, the effects of layer thickness and the annealing process on tensile strength were observed to be relatively minor. In the current experimental configuration, tensile strength increased from approximately 35 MPa at 20% infill to about 45 MPa at 60% infill. Santosh et al. documented tensile strength values rising from approximately 20 MPa at 25% infill to about 40 MPa at 100% infill [34]. Öteyaka et al. also reported that tensile strength increased from around 16 MPa at 20% infill to approximately 36 MPa at 100% infill in FDM-fabricated PLA samples [36]. The observed increase in tensile strength with increasing infill density was aligned with previously reported findings in the literature and clearly confirmed that infill density functions as the principal structural parameter controlling tensile performance. The highest elastic modulus value was obtained for sample S3 with 928.37 MPa, followed by S5 with 810.63 MPa and S9 with 771.52 MPa. In particular, samples S7 and S8 with a layer thickness of 0.20 mm exhibited the lowest elastic modulus values. This behavior was associated with the reduction in interlayer bonding quality due to increased layer thickness and the resulting lower stiffness in the elastic region. ANOVA results indicated that layer thickness had the greatest effect on elastic modulus, accounting for 48.17% of the total contribution. Infill density followed as the second most influential factor with a contribution of 27.83%, whereas the effect of annealing

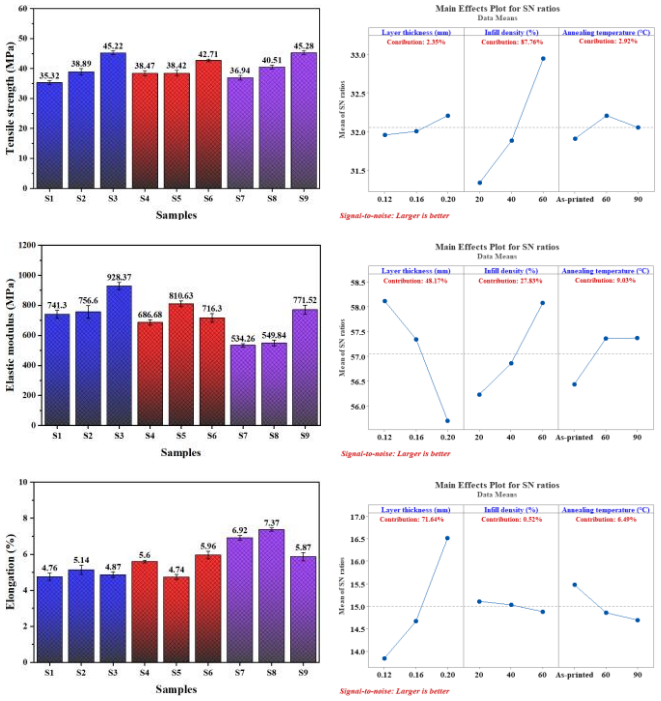

Figure 4. Tensile strength, elastic modulus, and elongation values of the samples, and their corresponding S/N graphs.

temperature was comparatively minor. These results stated that layer thickness, together with infill density, was a critical manufacturing parameter for the elastic modulus. This layer-thickness sensitivity of stiffness was also supported by published numerical data. Rodríguez-Panes et al. reported that when PLA layer height increased from 0.10 mm to 0.20 mm at constant infill, the elastic modulus changed from 1 GPa to 0.987 GPa, indicating a slight reduction in stiffness with increasing layer height [29]. Similarly, Rankouhi et al. also demonstrated that increasing layer thickness leads to a reduction in elastic modulus. In their study, samples printed at 0° raster orientation showed a decrease in elastic modulus from approximately 2200 MPa at 0.20 mm to about 1800 MPa at 0.40 mm [28]. In addition, ANOVA analysis in that study confirmed that layer thickness was the primary factor controlling elastic modulus. This finding is consistent with the dominant influence of layer thickness observed in the present study. The highest elongation values were obtained for samples S7 and S8 with a layer thickness of 0.20 mm, and these samples exhibited a more ductile deformation behavior. In contrast, samples with thinner layer thicknesses shown limited deformation capability due to increased structural rigidity, resulting in lower elongation values. Based on the S/N plots and ANOVA results, layer thickness was determined to be the most critical parameter affecting elongation, with a contribution ratio of 71.64%. These findings stated that ductility behavior was truly controlled by layer thickness. For the 40% infill samples (S2 and S8), elongation increased from approximately 5% to 7% as the layer thickness was raised from 0.12 mm to 0.20 mm. The effect of layer thickness observed in this study was also compared with tensile samples produced at similar infill ratios in previous research. Samykano et al. declared that increasing layer thickness altered deformation behavior and ductility in additively manufactured polymers. In their study, when the layer thickness increased from 0.4 mm to 0.5 mm, the average fracture strain increased from 0.069 to 0.083, clearly indicating that higher layer thickness promoted greater deformation capacity before failure [50]. These findings clearly demonstrated that thicker layers promoted increased elongation and a more ductile response.

When the tensile test results were evaluated together, it was specified that the tensile behavior varied in a nonlinear manner depending on the infill density and layer thickness. While the infill density had a dominant effect on tensile strength, the layer thickness controlled deformation-related properties such as elastic modulus and elongation, thereby the stiffness-ductility balance. Although the annealing treatment contribution was relatively limited, it could be stated that, under certain parameter combinations, it influenced the mechanical properties in a secondary yet guiding manner by reducing probable residual stresses.

The specific tensile strength graphs presented in Fig. 5 clearly demonstrated that mechanical performance should be evaluated not only in terms of absolute tensile strength but also in relation to the amount of material used. When sample weights were taken into account, the load-carrying capacity per unit mass was detected to be more efficient at low and intermediate infill densities. In contrast, at higher infill densities, the increased material content limited the gains in specific strength and resulted in a reduction in structural efficiency beyond a certain threshold. This finding indicated that porous structures could be more advantageous in terms of specific mechanical performance. Moreover, it showed that increases in absolute tensile strength did not always provide a weight-based advantage and that the combined evaluation of specific and absolute strength was a critical requirement in the design process [53], [54]. The increase in weight observed with increasing layer thickness, despite the gain in ductility, exerted a suppressive effect on specific tensile strength. However, appropriate combinations of layer thickness and infill density enabled both sufficient load-carrying capacity and weight efficiency to be achieved simultaneously. In addition, the annealing treatment was observed to indirectly support specific mechanical performance by improving interlayer interactions, particularly in low- and medium-density structures, and thus acted as a secondary but complementary parameter.

Table 3. ANOVA results for mechanical properties.

ANOVA results	Source	DF	Seq SS	Adj MS	F-Value	P-Value	Contribution (%)
Tensile strength	Layer thickness (mm)	2	0.1077	0.05383	0.34	0.747	2.35
	Infill density (%)	2	4.0130	2.00652	12.61	0.073	87.76
	Annealing temperature (°C)	2	0.1336	0.06682	0.42	0.704	2.92
	Error	2	0.3183	0.15916			6.96
	Total	8	4.5727				100.00
Elastic modulus	Layer thickness (mm)	2	9.072	4.5361	3.22	0.237	48.17
	Infill density (%)	2	5.241	2.6206	1.86	0.350	27.83
	Annealing temperature (°C)	2	1.700	0.8502	0.60	0.624	9.03
	Error	2	2.820	1.4098			14.97
	Total	8	18.833				100.00
Elongation	Layer thickness (mm)	2	11.1989	5.59946	3.36	0.230	71.64
	Infill density (%)	2	0.0820	0.04102	0.02	0.976	0.52
	Annealing temperature (°C)	2	1.0144	0.50719	0.30	0.767	6.49
	Error	2	3.3373	1.66866			21.35
	Total	8	15.6326				100.00

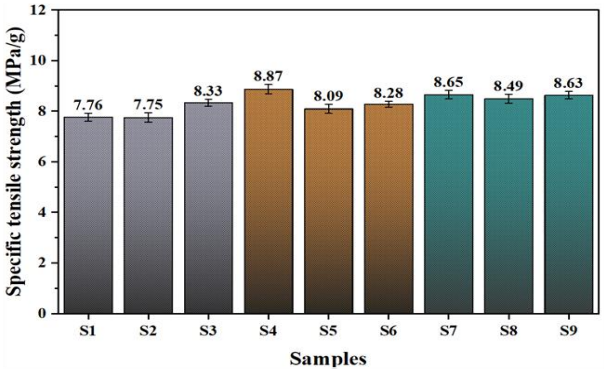

Figure 5. Specific tensile strength of samples.

B. Surface quality

Figure 6 presented the optical microscope images taken from the wide surfaces of all samples. Characteristic traces corresponding to molten filament deposition, extending parallel to the printing direction, were clearly observed on the sample surfaces. Moreover, with increasing layer thickness, these traces became more pronounced, the filament boundaries sharpened, and the density of microscale surface discontinuities increased.

Figure 7 presented the 3D profilometer images and the corresponding depth profiles obtained from the wide side surfaces of the FDM-fabricated tensile samples. Surface roughness measurements were carried out on these surfaces, where the layer boundaries were directly exposed and extended parallel to the printing direction. For all samples, a periodic peak–valley morphology aligned with the printing direction, corresponding to molten filament deposition, was clearly observed. With increasing layer thickness, the number of layers decreased, the surface traces associated with each layer became wider, and the height differences between consecutive layers (0.12, 0.16, and 0.20 mm) became more pronounced, as clearly evidenced in the 3D profilometer images. This geometric evolution led to the formation of sharper layer steps on the surface and, consequently, resulted in a direct increase in the measured surface roughness values.

Figure 8 presented the surface roughness values of all samples together with their corresponding S/N ratio plots. The ANOVA results for surface roughness values were also given in Table 4. S/N analyses were performed using the smaller is better approach for surface roughness. The highest surface roughness values were measured for the samples (S7, S8, and S9) with a layer thickness of 0.20 mm.

Analysis of the S/N graphs showed that surface roughness was predominantly affected by layer thickness, which accounted for

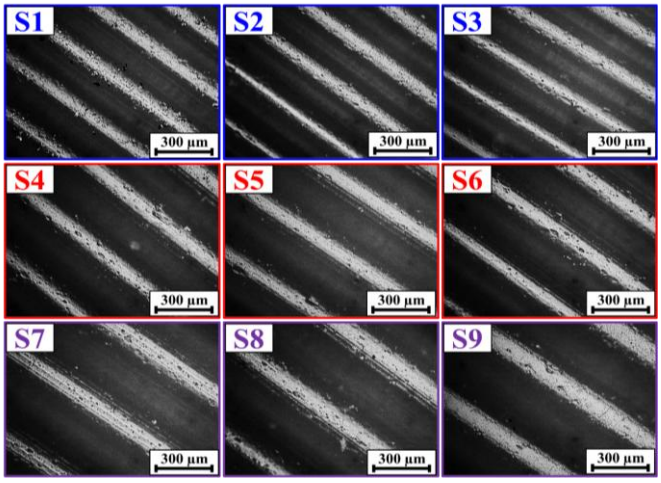

Figure 6. Optical microscope image of sample surfaces.

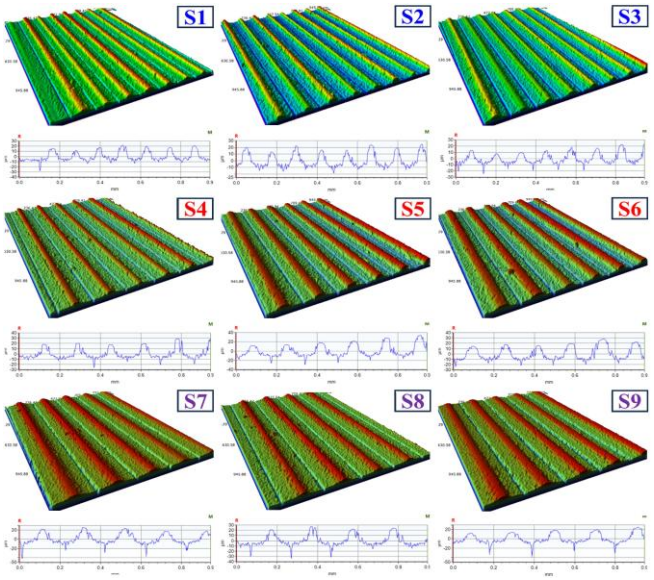

Figure 7. 3D profilometer image of sample surfaces.

84.73% of the overall contribution. In comparison, infill density and annealing treatment exhibited no notable influence on surface roughness. Although annealing did not show a statistically significant effect on Ra values, its role was evaluated within the overall processing framework. Annealing primarily influenced, probably, internal stress distribution and crystallinity, yet under the selected parameter combinations, its contribution remained limited compared to geometric factors. Surface roughness was predominantly controlled by layer-step formation during deposition. In this study, for samples printed at 20% infill density, increasing the layer thickness from 0.12 mm to 0.20 mm resulted in an increase in surface roughness from approximately 7 µm to about 11 µm. Similar quantitative trends were reported in previous studies. Vidakis et al. showed that increasing layer thickness from 0.10 mm to 0.25 mm led to an increase in average surface roughness from approximately 9 µm to about 15 µm in FDM-printed PLA samples [26]. These numerical findings were confirmed geometric deposition parameters dominate surface quality in FDM-fabricated components. This integrated evaluation of geometric and thermal parameters emphasized the importance of combined parameter evaluation in FDM-fabricated PLA components.

When the relationship between mechanical performance and surface roughness was evaluated together, it was determined that increasing layer thickness led to changes in both elastic modulus and elongation. With increasing layer thickness, microscale geometric irregularities caused the load transfer in the elastic region to become more heterogeneous, which resulted in a reduction in elastic stiffness. On the other hand, surface irregularities associated with increased surface roughness, together with variations in the interlayer bonding mechanism, had a pronounced effect on the elongation of the samples. The literature also reported that, in FDM-fabricated polymer structures, surface roughness played a decisive role in elastic stiffness and ductile deformation behavior, and that this effect

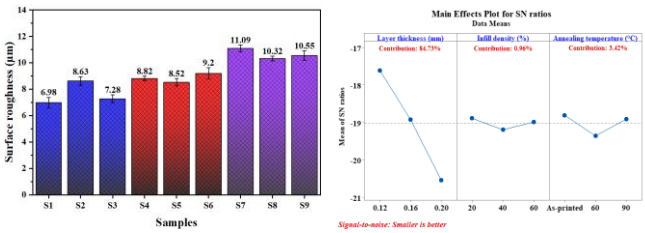

Figure 8. Surface roughness values of the samples and their corresponding S/N graphs.

Table 4. ANOVA results for surface roughness values.

ANOVA results	Source	DF	Seq SS	Adj MS	F-Value	P-Value	Contribution (%)
Surface roughness	Layer thickness (mm)	2	12.9428	6.47138	7.77	0.114	84.73%
	Infill density (%)	2	0.1460	0.07301	0.09	0.919	0.96%
	Annealing temperature (°C)	2	0.5217	0.26086	0.31	0.761	3.42%
	Error	2	1.6652	0.83258			10.90%
	Total	8	15.2756				100.00%

became more pronounced with increasing layer thickness [49], [55]. In this context, the obtained results demonstrated that surface topography was a critical parameter not only for surface quality but also for the stiffness–ductility balance.

IV. CONCLUSION

This study investigated how layer thickness, infill density, and annealing temperature influence the tensile performance and surface characteristics of PLA samples. Through the combined use of tensile testing, surface measurements, and Taguchi-based statistical methods, both the individual and interactive effects of key processing parameters on mechanical behavior and surface quality were quantitatively evaluated. The principal outcomes of the study are summarized below:

- The infill density was found to be the dominant factor influencing tensile strength, contributing 87.76% according to ANOVA results. Samples fabricated with a 60% infill density achieved the highest tensile strength, with values of approximately 43–45 MPa.
- Layer thickness played a dominant role in controlling deformation-related properties. It contributed 48.17% to the variation in elastic modulus and 71.64% to the variation in elongation, clearly demonstrating its dominant role in the stiffness–ductility balance of PLA samples. In addition, increasing the layer thickness led to a decrease in elastic modulus while enhancing elongation, indicating a shift from a more rigid and brittle behavior toward a more ductile mechanical response.
- Annealing treatment exhibited a secondary but beneficial influence, particularly by enhancing interlayer bonding under selected parameter combinations, although its direct effect on tensile strength remained limited.
- The evaluation of specific tensile strength revealed that increases in absolute tensile strength do not always translate into weight-efficient performance, highlighting the necessity of considering both absolute and specific metrics during design optimization.
- Surface roughness was strongly related to layer thickness, with a contribution ratio of 84.73%. Thicker layers led to more pronounced layer-step geometries and increased height differences on the surface, directly increasing Ra values.

Overall, the results demonstrated that the surface quality and mechanical performance of PLA components can be effectively tailored through controlled adjustment of production parameters. In this regard, the present findings provide a valuable design guideline for engineering components in which weight efficiency, mechanical performance, and surface integrity must be optimized simultaneously. Future studies may expand this framework by incorporating additional printing parameters, such as nozzle temperature, printing speed, raster orientation, and cooling conditions, together with multi-objective optimization approaches and application-specific performance criteria, to achieve a broader evaluation of parameter interactions in FDM-fabricated PLA components.

AUTHOR STATEMENT

Plagiarism Check—The article has been scanned with iThenticate and found to be compliant with the journal's plagiarism policy.
Conflict of Interest—There is no conflict of interest with any person/organization.
Ethics Committee Approval—Ethics committee approval is not required for this article.
Use of Artificial Intelligence Tools—In this study, ChatGPT-5.3 was used for grammar and spell checking. All content reflects the original contribution of the authors.
Funding—No institutional/financial support was received for this study.
Data availability—The data supporting the findings of this study were generated by the author(s) and may be obtained from the author(s) upon request.
CRediT Author Contribution—Methodology, Investigation, Writing - Original Draft (**Gökhan Haydarlar**); Conceptualization, Methodology, Investigation, Writing - Review & Editing (**Tevfik Oğuzhan Ergüder**); Conceptualization, Methodology, Investigation, Writing - Review & Editing, Visualization (**Semih Duran**).

REFERENCES

[1] Q. Yan, H. Dong, J. Su, J. Han, B. Song, Q. Wei, Y. Shi, "A review of 3D printing technology for medical applications", *Engineering*, 4(5), (2018), 729–742.
[2] S. Dağlı, "Investigation of the Bonding Performance of Parts Produced by FDM and SLA 3D Printing Methods", *Manufacturing Technologies and Applications*, 6(1), (2025), 100–110.
[3] M. M. Sofu, H. V. Özkavak, S. Bacak, M. Fenkli, "Comparison of Strength, Surface Quality and Cost of Different Additive Manufacturing Methods", *Manufacturing Technologies and Applications*, 4(1), (2023), 25–36.
[4] S. C. Joshi, A. A. Sheikh, "3D printing in aerospace and its long-term sustainability", *Virtual and physical prototyping*, 10(4), (2015), 175–185.
[5] T. Singh, S. Kumar, S. Sehgal, "3D printing of engineering materials: A state of the art review", *Materials today: proceedings*, 28, (2020), 1927–1931.
[6] A. Aimar, A. Palermo, B. Innocenti, "The role of 3D printing in medical applications: a state of the art", *Journal of healthcare engineering*, 2019(1), (2019), 5340616.
[7] P. Jain, A. M. Kuthe, "Feasibility study of manufacturing using rapid prototyping: FDM approach", *Procedia Engineering*, 63, (2013), 4–11.
[8] T. N. A. T. Rahim, A. M. Abdullah, H. Md Akil, "Recent developments in fused deposition modeling-based 3D printing of polymers and their composites", *Polymer Reviews*, 59(4), (2019), 589–624.
[9] İ. B. Yeter, H. Kenan, C. O. Azeloğlu, "Kafes geometriye sahip sandviç bir yapının mekanik özelliklerinin deneysel ve sayısal analizi", *Pamukkale Üniversitesi Mühendislik Bilimleri Dergisi*, 32(1), (2025), 23-34.
[10] M. I. Abd El Aal, M. M. Awd Allah, S. A. Abd Alaziz, M. A. Abd El-baky, "Biodegradable 3D printed polylactic acid structures for different engineering applications: effect of infill pattern and density", *Journal of Polymer Research*, 31(1), (2024), 4.
[11] M. Altuğ, Y. Yılmaz, "Examination of 3D printing parameters using machine learning", *Pamukkale Üniversitesi Mühendislik Bilimleri Dergisi*, to be published, doi:10.65206/pajes.91679.
[12] İ. B. Toprak, "Eriyik Yığma Modelleme Süreç Parametrelerinin Taguchi Tabanlı Gri İlişkisel Analiz Yöntemi ile Çoklu Yanıt Optimizasyonu", *Manufacturing Technologies and Applications*, 5(2), (2024), 89-103.
[13] M. M. Prabhakar, A. K. Saravanan, A. H. Lenin, K. Mayandi, P. S. Ramalingam, "A short review on 3D printing methods, process parameters and materials", *Materials Today: Proceedings*, 45, (2021), 6108–6114.
[14] A. K. Sood, R. K. Ohdar, S. S. Mahapatra, "Experimental investigation and empirical modelling of FDM process for compressive strength improvement", *Journal of Advanced Research*, 3(1), (2012), 81–90.
[15] Y. Kuruoğlu, M. Akgün, H. Demir, "Analysis and Optimization of Process Parameters Affecting on the Tensile Strength of PLA and Iron-Reinforced PLA Samples Fabricated by Fused Deposition Modeling Method", *Manufacturing Technologies and Applications*, 4(2), (2023), 72–80.

[16] M. Günay, S. Gündüz, H. Yılmaz, N. Yaşar, R. Kaçar, "PLA esaslı numunelerde çekme dayanımı için 3D baskı işlem parametrelerinin optimizasyonu", *Politeknik Dergisi*, 23(1), (2020), 73–79.

[17] Q. Guo, J. C. Crittenden, "An energy analysis of polylactic acid (PLA) produced from corn grain and corn stover integrated system", *Proceedings of the 2011 IEEE International Symposium on Sustainable Systems and Technology*, Chicago, IL, USA, 16-18 May 2011, 1–5.

[18] S. Demir, "3B yazıcı ile Poli laktik asit (PLA) esaslı numune üretiminde yazıcı parametrelerinin sertlik üzerindeki etkisi", *Pamukkale Üniversitesi Mühendislik Bilimleri Dergisi*, 30(2), (2024), 136–144.

[19] H. T. H. Nguyen, P. Qi, M. Rostagno, A. Feteha, S. A. Miller, "The quest for high glass transition temperature bioplastics", *Journal of Materials Chemistry A*, 6(20), (2018), 9298–9331.

[20] T. J. Suteja, A. Soesanti, "Mechanical properties of 3D printed polylactic acid product for various infill design parameters: a review", *Journal of Physics: Conference Series*, 1569(4), (2020), 042010.

[21] K. N. Gunasekaran, V. Aravinth, C. B. M. Kumaran, K. Madhankumar, S. P. Kumar, "Investigation of mechanical properties of PLA printed materials under varying infill density", *Materials Today: Proceedings*, 45, (2021), 1849–1856.

[22] M. H. Umer, M. B. Khan, M. Q. Zafar, G. Hussain, B. Ashfaq, M. U. Arshad, W. A. Lughmani, "Influence of process parameters on mechanical properties and surface roughness in fused filament fabrication: a comprehensive review", *Journal of the Brazilian Society of Mechanical Sciences and Engineering*, 47(6), (2025), 1–29.

[23] U. Raza, A. Ahmed, S. Waheed, M. Abid, M. Tahir, A. Zahid, A. Ahmed, M. Bilal, T. Hussain, G. Mustafa, "Recent advancements in fused deposition modeling", *Polymers for Advanced Technologies*, 36(1), (2025), e70028.

[24] K. Shergill, Y. Chen, S. Bull, "What controls layer thickness effects on the mechanical properties of additive manufactured polymers", *Surface and Coatings Technology*, 475, (2023), 130131.

[25] D. Syrlybayev, B. Zharylkassyn, A. Seisekulova, M. Akhmetov, A. Perveen, D. Talamona, "Optimisation of strength properties of FDM printed parts—A critical review", *Polymers*, 13(10), (2021), 1587.

[26] N. Vidakis, C. David, M. Petousis, D. Sagris, N. Mountakis, A. Moutsopoulou, "The effect of six key process control parameters on the surface roughness, dimensional accuracy, and porosity in material extrusion 3D printing of polylactic acid: Prediction models and optimization supported by robust design analysis", *Advances in Industrial and Manufacturing Engineering*, 5, (2022), 100104.

[27] M. Sharma, V. Sharma, P. Kala, "Optimization of process variables to improve the mechanical properties of FDM structures", *Journal of Physics: Conference Series*, 1240(1), (2019), 012061.

[28] B. Rankouhi, S. Javadpour, F. Delfanian, T. Letcher, "Failure analysis and mechanical characterization of 3D printed ABS with respect to layer thickness and orientation", *Journal of Failure Analysis and Prevention*, 16(3), (2016), 467–481.

[29] A. Rodríguez-Panes, J. Claver, A. M. Camacho, "The influence of manufacturing parameters on the mechanical behaviour of PLA and ABS pieces manufactured by FDM: A comparative analysis", *Materials*, 11(8), (2018), 1333.

[30] W. Kiński, P. Pietkiewicz, "Influence of the print layer height in FDM technology on the rolling force value and the print time", *Agricultural Engineering*, 23(4), (2019), 1-9.

[31] M. S. Anoop, P. Senthil, "Homogenisation of elastic properties in FDM components using microscale RVE numerical analysis", *Journal of the Brazilian Society of Mechanical Sciences and Engineering*, 41(12), (2019), 540.

[32] V. S. Jatti, S. V Jatti, A. P. Patel, V. S. Jatti, "A study on effect of fused deposition modeling process parameters on mechanical properties", *International Journal of Scientific & Technology Research*, 8(11), (2019), 689–693.

[33] S. Garg, A. Singh, Q. Murtaza, "Measuring the Impact of Infill Pattern and Infill Density on the Properties of 3D-Printed PLA via FDM", *Journal of Materials Engineering and Performance*, 34, (2025), 22597–22610.

[34] S. Santosh, M. S. S. Muthiah, K. S. Nishad, "Influence of infill density on the mechanical properties and fracture behavior of 3D-printed PLA+ components", *Macromolecular Research*, 33, (2025), 1407–1420.

[35] B. A. Aloyaydi, S. Sivasankaran, H. R. Ammar, "Influence of infill density on microstructure and flexural behavior of 3D printed PLA thermoplastic parts processed by fusion deposition modeling", *AIMS materials science*, 6(6), (2019), 1033-1048.

[36] M. Ö. Öteyaka, K. Aybar, H. C. Öteyaka, "Effect of infill ratio on the tensile and flexural properties of unreinforced and carbon fiber-reinforced polylactic acid manufactured by fused deposition modeling", *Journal of Materials Engineering and Performance*, 30(7), (2021), 5203–5215.

[37] P. K. Mishra, P. Senthil, S. Adarsh, M. S. Anoop, "An investigation to study the combined effect of different infill pattern and infill density on the impact strength of 3D printed polylactic acid parts", *Composites Communications*, 24, (2021), 100605.

[38] M. Vorkapić, I. Mladenović, T. Ivanov, A. Kovačević, M. S. Hasan, A. Simonović, I. Trajković, "Enhancing mechanical properties of 3D printed thermoplastic polymers by annealing in moulds", *Advances in Mechanical Engineering*, 14(8), (2022), 16878132221120736.

[39] R. A. Wach, P. Wolszczak, A. Adamus-Wlodarczyk, "Enhancement of mechanical properties of FDM-PLA parts via thermal annealing", *Macromolecular Materials and Engineering*, 303(9), (2018), 1800169.

[40] L. Yu, H. Liu, F. Xie, L. Chen, X. Li, "Effect of annealing and orientation on microstructures and mechanical properties of polylactic acid", *Polymer Engineering & Science*, 48(4), (2008), 634–641.

[41] F. Kartal, A. Kaptan, "Effects of annealing temperature and duration on mechanical properties of PLA plastics produced by 3D Printing", *European Mechanical Science*, 7(3), (2023), 152–159.

[42] R. V. Pazhamannil, N. Krishnan C, G. P, A. Edacherian, "Investigations into the effect of thermal annealing on fused filament fabrication process", *Advances in Materials and Processing Technologies*, 8(2), (2022), 710–723.

[43] I. A. Reis, P. I. Cunha Claro, A. L. Marcomini, L. H. Capparelli Mattoso, S. P. da Silva, A. R. de Sena Neto, "Annealing and crystallization kinetics of poly (lactic acid) pieces obtained by additive manufacturing", *Polymer Engineering & Science*, 61(7), (2021), 2097–2104.

[44] N. Jayanth, K. Jaswanthraj, S. Sandeep, N. H. Mallaya, S. R. Siddharth, "Effect of heat treatment on mechanical properties of 3D printed PLA", *Journal of the Mechanical Behavior of Biomedical Materials*, 123, (2021), 104764.

[45] H. Kang, Y. Li, M. Gong, Y. Guo, Z. Guo, Q. Fang, X. Li, "An environmentally sustainable plasticizer toughened polylactide", *RSC advances*, 8(21), (2018), 11643–11651.

[46] S. Singh, A. Rajeshkannan, S. Feroz, A. K. Jeevanantham, "Effect of normalizing on the tensile strength, shrinkage and surface roughness of PLA plastic", *Materials Today: Proceedings*, 24, (2020), 1174–1182.

[47] H. Gonabadi, A. Yadav, S. J. Bull, "The effect of processing parameters on the mechanical characteristics of PLA produced by a 3D FFF printer", *The International Journal of Advanced Manufacturing Technology*, 111(3), (2020), 695–709.

[48] Y. Y. Aw, C. K. Yeoh, M. A. Idris, P. L. Teh, K. A. Hamzah, S. A. Sazali, "Effect of printing parameters on tensile, dynamic mechanical, and thermoelectric properties of FDM 3D printed CABS/ZnO composites", *Materials*, 11(4), (2018), 466.

[49] Y. Zhao, Y. Chen, Y. Zhou, "Novel mechanical models of tensile strength and elastic property of FDM AM PLA materials: Experimental and theoretical analyses", *Materials & Design*, 181, (2019), 108089.

[50] M. Samykano, S. K. Selvamani, K. Kadirgama, W. K. Ngui, G. Kanagaraj, K. Sudhakar, "Mechanical property of FDM printed ABS: influence of printing parameters", *The International Journal of Advanced Manufacturing Technology*, 102(9), (2019), 2779–2796.

[51] S. Valvez, A. P. Silva, P. N. B. Reis, F. Berto, "Annealing effect on mechanical properties of 3D printed composites", *Procedia Structural Integrity*, 37, (2022), 738–745.

[52] X. Zhao, J. Liu, J. Li, X. Liang, W. Zhou, S. Peng, "Strategies and techniques for improving heat resistance and mechanical performances of poly (lactic acid)(PLA) biodegradable materials", *International Journal of Biological Macromolecules*, 218, (2022), 115–134.

[53] M. Ö. Öteyaka, F. H. Çakir, M. A. Sofuoğlu, "Effect of infill pattern and ratio on the flexural and vibration damping characteristics of FDM printed PLA samples", *Materials Today Communications*, 33, (2022), 104912.

[54] E. Kaya, İ. Bayar, A. F. Akpınar, "Dolgu desenlerinin ve oranlarının ergiyik biriktirme modellemede PLA malzemesinin mekanik performansına olan etkisi", *Niğde Ömer Halisdemir Üniversitesi Mühendislik Bilimleri Dergisi*, 13(3), (2024), 792–798.

[55] S. Ekşi, C. Karakaya, "Effects of process parameters on tensile properties of 3D-Printed PLA parts fabricated with the FDM method", *Polymers*, 17(14), (2025), 1934.